

# UC Davis

## UC Davis Previously Published Works

### Title

Compact Wide Stopband Bandpass Filter on Multilayer Organic Substrate

### Permalink

<https://escholarship.org/uc/item/6xh9c0hh>

### Journal

IEEE Microwave and Wireless Components Letters, 24(3)

### ISSN

1531-1309

### Authors

Ta, Hai Hoang  
Pham, Anh-Vu

### Publication Date

2014-03-01

### DOI

10.1109/lmwc.2013.2293672

Peer reviewed

# Compact Wide Stopband Bandpass Filter on Multilayer Organic Substrate

Hai Hoang Ta, *Member IEEE*, Anh-Vu Pham, *Senior Member*

**Abstract**— We present the design and development of a compact wide stopband bandpass filter using novel quasi-lumped LC resonators on a defected ground structure. The resonators are built on a multilayer organic substrate and are coupled to external circuits by shunt-inductive impedance inverters. Experimental results show that the filter has a center frequency of 960 MHz and a 3-dB fractional bandwidth of 8%. The filter has a wide stopband that has an out-of-band rejection of better than 30 dB up to five times of the center frequency. The size of the filter is 5.4 mm x 27 mm or  $0.027\lambda_g \times 0.132\lambda_g$ , where  $\lambda_g$  is guided wavelength at 960 MHz.

**Index Terms**— Band-pass Filter, Wide Stopband, Quasi-lumped, Multilayer.

## I. INTRODUCTION

BAND-PASS filters play an important role in many communication circuits. Band-pass filters with wide stopband and high selectivity are desirable to improve system performance. An ideal filter is expected to be free of spurious pass-bands. Conventional filter designs that are based on distributed components usually suffer from unwanted spurious responses. There are many techniques that have been proposed to design bandpass filters that have wide stopband [1 - 5]. In [1], the stopband of a conventional J-inverter filter is widened with the assistance of open transmission line stubs and interdigitated capacitors. In [2], the rejection of multi-spurious pass bands in a parallel-coupled-line microstrip bandpass filter is achieved by using “Wiggly-line” structures. In [3], the suppression of spurious responses in the stopband is realized by choosing the constitutive resonators that has the same fundamental frequency, but staggering higher order resonant frequencies. In [4], wide-stopband microstrip bandpass filter is designed by using quarter-wavelength shorted coupled-lines. In [5], a defected ground structure (DGS) is deployed to realize a wide-stopband coupled-line bandpass filter.

In this letter, we present the development of a compact, wide-stopband bandpass filter using novel quasi-lumped LC resonators. The equivalent circuit of the quasi-lumped LC resonators consists of a capacitor in series with an inductor. The capacitor is formed by a metal-insulator-metal (MIM) structure while the inductance of the series inductor is dependent on the size of the rectangular-shape DGS on the

ground plane. The filter is implemented on a thin-film, multilayer Liquid Crystal Polymer (LCP) substrate that has 3 metal layers and 2 dielectric layers. The experimental results show that the measurement is well correlated with the EM simulation. The filter has the smallest size while achieving a comparable stopband performance in comparison with other published wide-stopband bandpass filters. Other reports on compact filters on LCP can be found in [12-14] which show great potential of using LCP in compact RF/microwave passive component designs.

## II. BANDPASS FILTER DESIGN

### A. MIM capacitor on a defected ground structure (DGS)

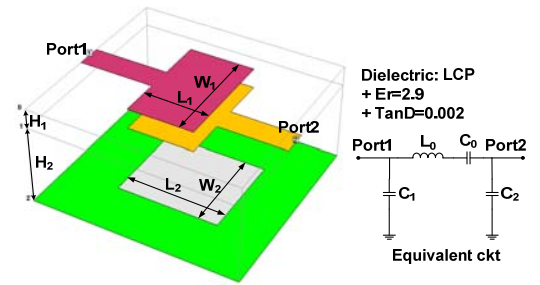


Fig. 1 3-dimensional view and lumped equivalent circuit of a MIM capacitor on a DGS

An MIM capacitor on a rectangular-shape DGS and its lumped equivalent circuit is presented in Fig. 1. The MIM capacitor is realized on a 3-metal layer LCP substrate that has a dielectric constant of 2.9 and a loss tangent of 0.002. The dielectric thicknesses are  $H_1 = 2$  mil and  $H_2 = 12$  mil. The MIM capacitor has dimensions  $L_1$  and  $W_1$  while the dimensions of the rectangular DGS are  $L_2$  and  $W_2$ . In the equivalent circuit of the MIM capacitor,  $C_0$  is the main capacitance of the MIM capacitor.  $C_1$  and  $C_2$  are parasitic capacitances which are usually much smaller than  $C_0$  can be negligible at low frequency ranges. The series inductance  $L_0$  is mainly from the DGS [6].

$C_0$  can be approximated by the equation:

$$C_0 = \epsilon_r \epsilon_0 \frac{W_1 L_1}{H_1} \quad (1)$$

where  $\epsilon_r=2.9$  is the dielectric constant of the dielectric layer between the top- and second-layer conductor;  $\epsilon_0=8.854 \times 10^{-12}$  is the permittivity of free-space.

In this configuration,  $C_1$  and  $C_2$  are  $\ll C_0$  and can be negligible.  $L_0$  can be determined by the equation:

$$L_0 = \frac{1}{\omega_0^2 C_0} \quad (2)$$

Manuscript received on July 25th, 2013 and revised on July 25th, 2013. This work is supported in part by Vietnam Education Foundation, and Agilent Technologies. H.H. Ta, and A.V. Pham are with the School of Electrical and Computer Engineering, University of California at Davis, Davis, CA 95616 USA (email: [hhta@ucdavis.edu](mailto:hhta@ucdavis.edu))

where  $\omega_0$  is the self-resonant frequency of the MIM capacitor.  $\omega_0$  can be determined by looking at the imaginary part of the input impedance at port 1 of the capacitor while port 2 is shorted.  $\omega_0$  is the frequency where the imaginary part equal to zero.

High frequency structure simulator (HFSS) [7] is used to model and evaluate the input impedance of the MIM capacitor. From this input impedance, the resonant frequency  $\omega_0$  of the MIM capacitor can be determined. Once  $\omega_0$  is known,  $C_0$  and  $L_0$  can be calculated from equations (1) and (2). For fixed values of  $W_1$  and  $L_1$ ,  $C_0$  is almost constant while  $L_0$  is proportional to both  $W_2$  and  $L_2$ . Fig. 2 shows the variation of  $L_0$  as  $W_2$  and  $L_2$  change. The data were taken with  $L_1=105$  mil and  $W_1=175$  mil. With these dimensions, the value of  $C_0$  is  $\sim 6$ pF.

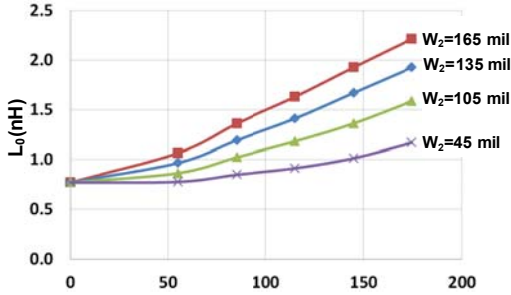


Fig.2. Variation of  $L_0$  as  $L_2$  and  $W_2$  change

### B. Bandpass filter design

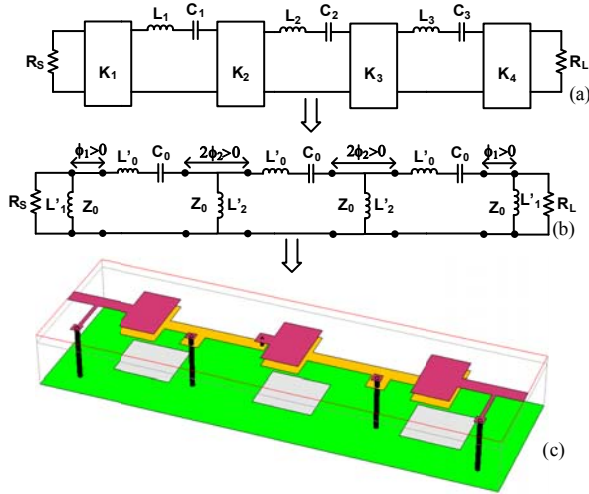


Fig. 3. Circuit schematic and realization of the band-pass filter

Fig.3. shows the circuit schematics and the 3-Dimensional view of the band-pass filter realized on a multilayer dielectric substrate. The filter is based on direct-coupled resonators with impedance inverters and series LC resonators as shown in Fig. 3(a). The values of the characteristic impedance of the inverters  $K_j$  ( $j=1-4$ ) and the series capacitances and inductances  $C_j$  and  $L_j$  ( $j=1-4$ ) are determined by using the equations in [8]. The filter is designed to have 3<sup>rd</sup>-order 0.1-dB-ripple Tchebycheff response, a center frequency of 960 MHz and a 3-dB bandwidth of 5%. Impedance inverter transformations are used to make the series LC resonators become identical. The equations for these transformations can

be found in [9]. The impedance inverters are realized by a shunt inductor, series transmission line elements and series negative inductors as shown in Fig. 3(b). The method to realize these impedance inverters can be found in [10]. The series LC resonators are realized by using DGS MIM capacitors on a multilayer dielectric substrate. From the value of  $C_0$ , the dimensions  $W_1$  and  $L_1$  can be determined. From analysis of a DGS MIM capacitor, the values of  $W_2$  and  $L_2$  can be chosen to obtain the series inductance  $L'_0$ . Fig. 3(c) represents the implementation of the filter. Tables 1 and 2 summarize the values of inductances, capacitances, transmission line electrical lengths and dimensional parameters of the DGS MIM capacitor.

TABLE I  
SUMMARY VALUES OF INDUCTANCES, CAPACITANCES AND ELECTRICAL LENGTHS

$L'_0$ (nH)	$C_0$ (pF)	$L'_1$ (nH)	$L'_2$ (nH)	$\phi_1$ (degree)	$\phi_2$ (degree)
1.8	6.2	1.7	0.25	2.9	7.6

TABLE II  
SUMMARY OF THE RESONATOR'S DIMENSIONS

$W_1$ (mm)	$L_1$ (mm)	$W_2$ (mm)	$L_2$ (mm)
4.45	2.67	3.68	4.19

The shunt inductors are realized by short-circuited transmission line stubs. The series transmission elements have the same characteristic impedance of 50 ohm. Fabricated prototype of the filter is shown in Fig. 4. Coplanar wave guide pads are added for probe measurement. The total size of the filter without probe pads is 5.4 mm x 27 mm.



Fig. 4. Filter fabricated prototype

### III. EXPERIMENTAL RESULTS

The filter is modeled in high frequency structure simulator (HFSS) [7]. Electrical performance of the filter was measured on a Cascade Microtech RF probe station with an Agilent E8364 2-port network analyzer. The probes were calibrated using standard TRL calibration on a Picoprobe CS-9 substrate [11].

The simulated and measured results of S11 and S21 of the filter are shown in Fig. 5. As can be seen, the measurement is well correlated with the simulation. Based on measured results, the filter has a center frequency at 960 MHz, a 3-dB bandwidth of 8%. The measured insertion loss at the center frequency is 4.0 dB. The loss is mainly from conductor and radiation losses. The radiation loss is caused by the DGS as well as the air exposure of the MIM capacitor metal pads. This loss can be reduced by putting the filter inside an enclosed metal package. As can be seen in Fig. 5a, the in-band insertion can be improved by  $\sim 1$ dB if the filter is enclosed in a metal package. **The enclosed metal package is described in Fig. 6.**

The filter has an out-of-band rejection of better than 30 dB up to five times of the center frequency. Table III shows the comparisons of this filter with other published wide-stopband bandpass filters.

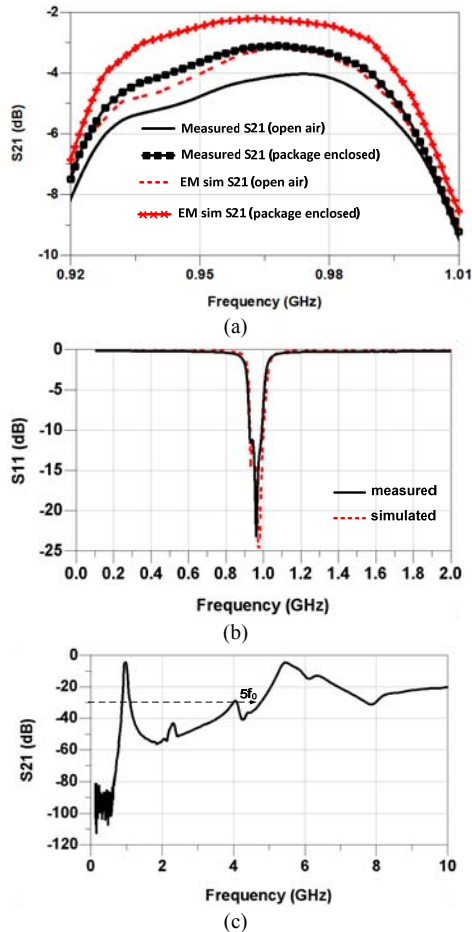


Fig. 5. Measured response of the filter. (a) – In-band insertion loss; (b) – Return loss; (c) – Wideband insertion loss

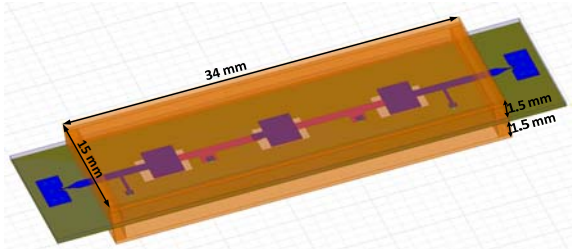


Fig. 6. Enclosed the filter by a metal package.

TABLE III  
BANDPASS FILTER COMPARISONS

Filters	$f_0$ / FBW	Order/ Loss	Size	Stopband
[1]	1 GHz/ 18%	5 <sup>th</sup> / 0.9dB	$0.17\lambda_g \times$ $0.18\lambda_g$	26 dB up to $22f_0$
[2]	2.5 GHz/ 10%	7 <sup>th</sup> / 2.0 dB	$0.37\lambda_g \times$ $2\lambda_g$	30 dB up to $7f_0$
[3]	1.5 GHz/ 5.6%	4 <sup>th</sup> / 2.7 dB	$0.23\lambda_g \times$ $0.97\lambda_g$	30 dB up to $5.4f_0$
[4]	2.35 GHz/ 8%	3 <sup>rd</sup> / 2.1 dB	$0.18\lambda_g \times$	20 dB up

	6.54%		$0.26\lambda_g$	to $4.5f_0$
<b>This work</b>	960 MHz/ 8%	3 <sup>rd</sup> / 4.0 dB	$0.03\lambda_g \times$ $0.13\lambda_g$	30 dB up to $5f_0$

#### IV. CONCLUSION

We present the development of a compact wide stopband bandpass filter using novel quasi-lumped LC resonators on a defected ground structure. Experimental results show that the filter has a pass band at a center frequency of 960 MHz with a 3-dB fractional bandwidth of 8%. The filter has a wide stopband that has an out-of-band rejection better than 30 dB up to five times of the center frequency. The measurements are well matched with the EM simulations. The size of the filter is 5.4 mm x 27 mm or  $0.027\lambda_g \times 0.132\lambda_g$ , where  $\lambda_g$  is guided wavelength at 960 MHz.

#### ACKNOWLEDGMENT

This work is supported in part by Vietnam Education Foundation and Agilent Technologies.

#### REFERENCES

- [1] Ching-Wen Tang; Yen-Kuo Hsu, "A Microstrip Bandpass Filter With Ultra-Wide Stopband," *IEEE Transactions on microwave theory and techniques*, Vol. 56, No. 6, pp 1468 – 1472, 2008.
- [2] Lopetegui, T.; Laso, M.A.G.; Falcone, F.; Martin, F.; Bonache, J.; Garcia, J.; Perez-Cuevas, L.; Sorolla, M.; Guglielmi, M., "Microstrip "Wiggly-Line" Bandpass Filters With Multispurious Rejection," *IEEE Microwave and Wireless Components Letters*, vol. 14, no. 11, pp. 531-533, 2004.
- [3] Chi-Feng Chen; Ting-Yi Huang; Ruey-Beei Wu, "Design of Microstrip Bandpass Filters With Multiorder Spurious-Mode Suppression" *IEEE Transactions on microwave theory and techniques*, Vol. 53, No. 12, pp 3788 - 3793, 2005.
- [4] Xun Luo; Huizhen Qian; Jian-Guo Ma; Kiat Seng Yeo, "A Compact Wide Stopband Microstrip Bandpass Filter Using Quarter-Wavelength Shorted Coupled-lines" *Proc. Asia-Pacific Microw. Conf.*, 2010, pp. 1142 – 1145.
- [5] Jun-Seok Park; Jun-Sik Yun; Dal Ahn, "A Design of the Novel Coupled-Line Bandpass Filter Using Defected Ground Structure With Wide Stopband Performance" *IEEE Transactions on microwave theory and techniques*, Vol. 50, No. 9, pp 2037 - 2043, 2002.
- [6] Chul-Soo Kim; Jun-Seok Park; Dal Ahn; Jae-Bong Lim, "A novel 1-D periodic defected ground structure for planar circuits" *Microwave and Guided Wave Letters, IEEE*, Vol. 10, No. 4, pp 131 - 133, 2000.
- [7] [Online]. Available: <http://www.ansoft.com/products/hf/hfss/>
- [8] G. Mattaei, L Young, EMT Jones, *Microwave Filters, Impedance-Matching Networks, and Coupling Structures*, Artech House, Dedham, Mass, USA, 1980.
- [9] Robert E. Collin, *Foundations for Microwave Engineering*, 2<sup>nd</sup> edition, A John Wiley & Sons, Inc., 2000.
- [10] [4-2] Levy, R., "A Generalized Design Technique for Practical Distributed Reciprocal Ladder Networks," *IEEE Transactions on microwave theory and techniques*, Vol. 21, No. 8, pp 519 – 526, 1973.
- [11] [Online]. Available: <http://www.ggb.com/calsel.html>
- [12] Hao, Z.-C., Hong, J.S., "Compact ultra-wideband bandpass filter using broadside coupled hairpin structures on multilayer liquid crystal polymer substrate", *Electronics Letters*, Vol. 44, No. 20, pp. 1197-1198, 2008.
- [13] Ta, H.H., Pham, A.-V., "Dual Band Band-Pass Filter With Wide Stopband on Multilayer Organic Substrate", *IEEE Microwave and Wireless Components Letters*, Vol. 23, No. 4, pp. 193-195, 2013.
- [14] Zhang-Cheng Hao, Jia-Sheng Hong, "Compact Wide Stopband Ultra Wideband Bandpass Filter Using Multilayer Liquid Crystal Polymer Technology", *IEEE Microwave and Wireless Components Letters*, VOL. 19, NO. 5, MAY 2009.